PHYSICAL REVIEW B **85**, 045131 (2012)

Magnetic phase diagram of MnSi in the high-field region

S. V. Demishev,* V. V. Glushkov, I. I. Lobanova,† M. A. Anisimov, V. Yu. Ivanov, T. V. Ishchenko, M. S. Karasev, N. A. Samarin, N. E. Sluchanko, V. M. Zimin, and A. V. Semeno

A. M. Prokhorov General Physics Institute of the RAS, 38 Vavilov Street, 119991 Moscow, Russia

(Received 26 December 2011; published 30 January 2012)

The high-field region of the magnetic phase diagram of MnSi is probed by magnetization, resistivity, and magnetoresistance measurements carried out in the temperature range 1.8–300 K for magnetic fields up to 8 T. It is shown that the phase boundary between the paramagnetic (PM) phase and the spin-polarized (SP) phase has no positive slope as was suggested previously, and appears to be practically vertical at the transition temperature $T_c \sim 30$ K. We argue that the broad maxima of the resistivity and magnetization derivative, which develop in the range $T > T_c$, are determined by the specific form of functional dependences of these quantities in the PM phase and do not correspond to any "diffuse" SP-PM transition. A universal relation between magnetoresistance and magnetization $\Delta\rho/\rho = -a_0 M^2$ found in the PM phase of MnSi is shown to hold in a wide temperature and magnetic field range where magnetoresistance varies by more than two orders of magnitude. The analysis of the transport and magnetic resonance data favors the explanation of the magnetic properties of MnSi by Heisenberg-type localized magnetic moments rather than within the magnetism of itinerant electrons. A low-temperature anomaly at $T \sim 15$ K corresponding to the features of magnetoresistance and g factor is reported.

DOI: 10.1103/PhysRevB.85.045131 PACS number(s): 75.30.Kz, 75.50.Cc, 75.47.−m, 76.30.−v

I. INTRODUCTION

Manganese monosilicide, MnSi, has attracted attention for decades as an example of an itinerant magnet with helicoidal ordering.[1–8] The onset of the quantum criticality under high pressure[9–11] together with the formation of the skyrmion state[12,13] and topological Hall effect in the so-called A phase[14] lie in the focus of modern studies of this material. All these interesting phenomena are observed in moderate (less than 1 T) magnetic fields in the vicinity of the magnetic transition.

According to magnetic, transport, and neutron scattering data,[1–14] the transition to the helical state in zero magnetic field occurs at the critical temperature $T_{c0} \sim 29$ K. The increase of magnetic field B at $T < T_{c0}$ results in a sequence of phase transitions from helical to conic structure at $B \sim 0.1$ T and then from conical to ferromagnetic spin alignment at $B = B_c \sim 0.6$ T.[2] The latter magnetic state is also referred as the spin-polarized (SP) phase.[15] The mostly debated A phase exists in a narrow interval of temperatures (from $0.97T_{c0}$ to T_{c0}) and magnetic fields ($0.1 < B < 0.2$ T).[14]

The region $B > B_c$ is considered to be less interesting as long as only the transition from PM to SP phase is expected in the high-field range. It was earlier suggested from AC magnetic susceptibility $\chi(B,T)$ data[15] that (i) this PM-SP transition in a fixed magnetic field corresponds to a broad maximum of $\chi(B = \text{const}, T)$, (ii) the phase boundary $B_{SP}(T)$ has a positive slope, and (iii) the PM-SP transition is smooth and should be considered as a crossover phenomenon rather than a sharp transition. However, some recent results show that the high-field region of the MnSi magnetic phase diagram deserves more attention. For example, high-frequency electron spin resonance (ESR) data[16] indicate that at $B \sim 2$ T the physical picture of dynamic magnetic properties surprisingly more closely matches Heisenberg-type localized magnetic moments and is hardly consistent with the standard understanding of MnSi as an itinerant magnet.[1] Probably this behavior reflects the field-induced suppression of spin fluctuations dominating in the low-magnetic-field region, which may affect the PM-SP transition.

In the present work the phase boundary between PM and SP phases has been probed by means of resistivity, magnetoresistance, and magnetization measurements. The ESR data reported in Ref. 16 were revised and considered together with the aforementioned physical properties. We argue that the $B_{SP}(T)$ phase boundary located at $T_c \sim 30$ K in magnetic fields up to $B \sim 8$ T is almost vertical (field independent), in contrast to previous findings. Moreover, this transition may be considered to be sharp, although some physical properties demonstrate broad peculiarities. It is found that magnetoresistance in the PM phase of MnSi is controlled by magnetic scattering on the Heisenberg-type localized magnetic moments and may be quantitatively described by the Yosida model.[17] The low-temperature anomaly, which seems to correspond to a transition at $T \sim 15$ K inside the SP phase, is examined.

II. EXPERIMENTAL DETAILS

Single crystals of MnSi were grown by the Bridgman method from a stoichiometric melt. The quality of crystals was controlled by x-ray and chemical analysis. The resistivity at $B = 0$ and magnetization data for the samples studied were very close to the MnSi characteristics reported previously in Refs. 18 and 19. The transition temperature in zero magnetic field was $T_{c0} = 29.15 \pm 0.03$ K. Temperature and field dependences of the resistivity $\rho(B,T)$ were measured by the standard DC four-probe technique in the temperature range 1.8–300 K for magnetic fields up to 8 T. The accuracy of temperature stabilization in the field scans at $T = \text{const}$ was better than 0.01 K. The magnetization data in magnetic fields up to 5 T were obtained with the help of a superconducting quantum interference device (SQUID) magnetometer (Quantum Design MPMS-5). The original experimental technique for studying magnetic resonance, which allows one to find the absolute values of the oscillating part of magnetization, is described

in previous papers.[16,20,21] The magnetic field was applied along the ⟨100⟩ direction for both resistivity and magnetization measurements, while current was directed parallel to the ⟨011⟩ axis of the MnSi crystal. The test measurements performed for various orientations of magnetic field showed no anisotropy of transport and magnetic properties within the experimental accuracy.

III. RESISTIVITY, MAGNETIZATION, AND MAGNETORESISTANCE DATA

The temperature dependence of resistivity $\rho(T)$ for the samples studied is shown in Fig. 1(a). The magnitude of the resistivity jump at the magnetic transition $\Delta\rho_0$ is about $\Delta\rho_0/\rho(T_{c0}) \approx 2.5\%$ [inset in Fig. 1(a)]. Following Ref. 18 it is convenient to analyze the derivative $\partial\rho/\partial T$ [Fig. 1(b)]. In zero magnetic field, the $\partial\rho/\partial T$ temperature dependence demonstrates a universal structure consisting of a narrow peak B superimposed by a broad maximum A. This type of the $\partial\rho/\partial T$ curve, which is typical for various physical properties measured in the vicinity of magnetic phase transition, has been earlier examined in detail by Stishov *et al.*[18] Although peak B is unambiguously related to the magnetic transition at T_c, the nature of the broad maximum A is not completely clarified in the available literature.

The increase of the magnetic field to 0.5 T induces broadening and shifting of peak B to lower temperatures, so

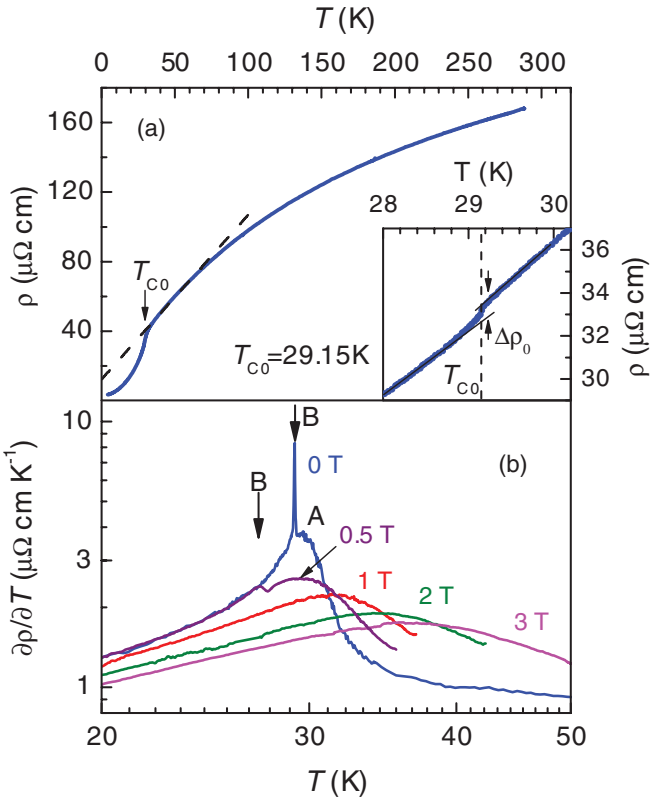

FIG. 1. (Color online) Temperature dependences of zero-field resistivity (a) and the derivatives $\partial\rho/\partial T$ calculated from the experimental data in various magnetic fields (b) for MnSi. The dashed line in panel (a) denotes the approximation used in simulations (Sec. V). The inset shows the jump in resistivity in the vicinity of T_{c0}.

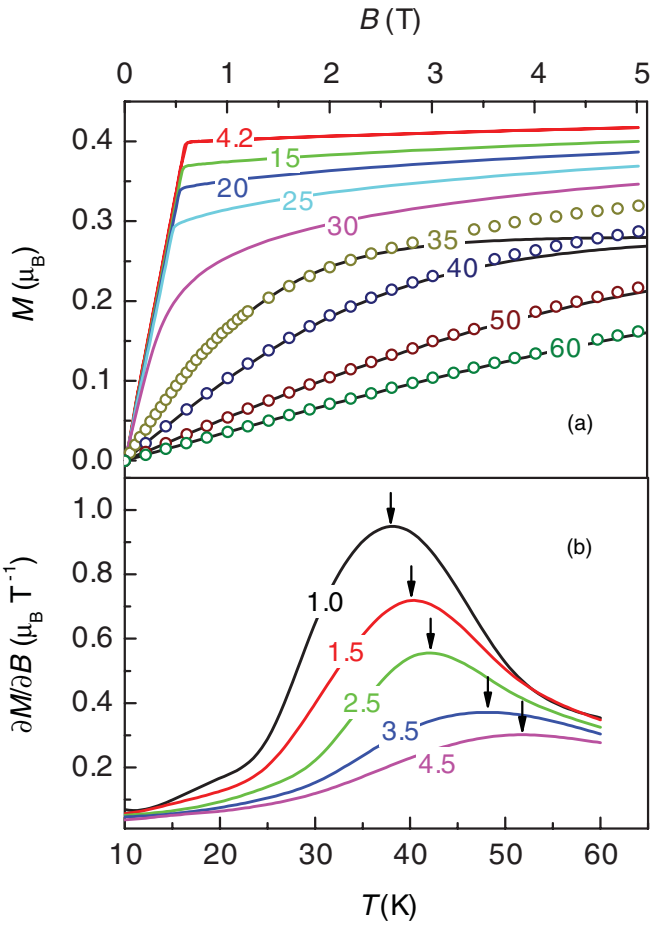

FIG. 2. (Color online) Magnetization M in μ_B per Mn ion (a) and derivatives $\partial M/\partial B$ (b) of MnSi. Numbers on the curves correspond to temperature in K in panel (a) and to magnetic field in T in panel (b). In panel (a) open circles for $T \geqslant 35$ K correspond to experimental data, while black lines are approximations used in numerical simulations (Sec. V). Experimental $M(B)$ data for $T \leqslant 30$ K are denoted by solid lines. In panel (b) arrows mark positions of the $\partial M/\partial B$ maxima.

that this feature is not observed for $B > 1$ T [Fig. 1(b)]. At the same time the maximum A shifts to higher temperatures at higher magnetic fields, and this feature becomes more wide and shallow [Fig. 1(b)]. This behavior qualitatively agrees with that reported previously for the susceptibility of MnSi.[15]

The field dependences of MnSi magnetization M at various temperatures are shown in Fig. 2(a). These data are in good agreement with the results reported in the literature, including the saturation value at liquid-helium temperatures, $M \sim 0.4\mu_B$/Mn. The accuracy of the magnetization $M(B,T)$ measurements performed in the temperature/magnetic field domain of 4.2–60 K at 5 T has allowed us to find temperature dependences of the derivative $\partial M/\partial B$ for various magnetic fields. It is obviously seen from the data of Fig. 2(b) that this effective susceptibility exhibits a maximum that broadens and shifts to higher temperatures when magnetic field increases. The positions of the maximum [arrows in Fig. 2(b)] are in fair agreement with the previous data.[15] It is worth noting that the maximum of $\partial M/\partial B$ should correspond to the transition from the SP to PM phase according to Ref. 15.

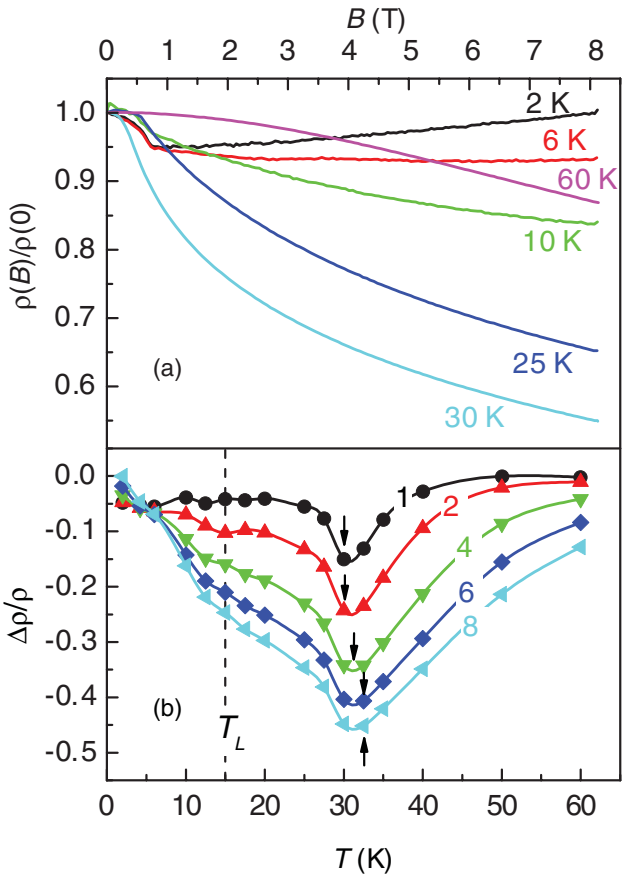

FIG. 3. (Color online) Field (a) and temperature (b) dependences of magnetoresistance in MnSi. In panel (b) numbers near curves correspond to magnetic field in T. Arrows mark the magnetoresistance minima and the dashed line indicates the position of the low-temperature anomaly.

Magnetoresistance is another quantity that may indicate a position of the PM-SP phase boundary. We found that for MnSi the magnetoresistance $\Delta\rho/\rho = \rho(B)/\rho(0) - 1$ is negative in magnetic fields up to 8 T [Fig. 3(a)]. For $T < 30$ K there are kinks on the field dependences $\Delta\rho/\rho = f(B, T = \text{const})$ marking positions of the known phase boundaries in the low-field ($B < 0.6$ T) region of the magnetic phase diagram. The temperature cuts $\Delta\rho/\rho = f(B = \text{const}, T)$ show broad minima in the vicinity of T_c [Fig. 3(b)]. However, the characteristic temperature of the magnetoresistance minima does not significantly depend on magnetic field. For $B < 2$ T it is located at $T \sim 30$ K, and the position of this feature changes by ~1 K only when the magnetic field reaches 6–8 T [Fig. 3(b)]. This structure of $\Delta\rho/\rho = f(B = \text{const}, T)$ was earlier reported but not examined in detail.[3]

The points corresponding to various extrema for $\partial\rho/\partial T$, $\partial M/\partial B$, and $\Delta\rho/\rho$ are put together in the magnetic phase diagram of MnSi (Fig. 4). It is interesting that the position of peak B in the magnetic field (red crosses in Fig. 4) perfectly coincides with the phase boundary between conical and SP phases. The situation is completely different for the broad features found in the high-field region of the magnetic phase diagram (Figs. 1–3). Contrary to the phase boundaries dividing helical, conical, and spin-polarized phases, where the changes

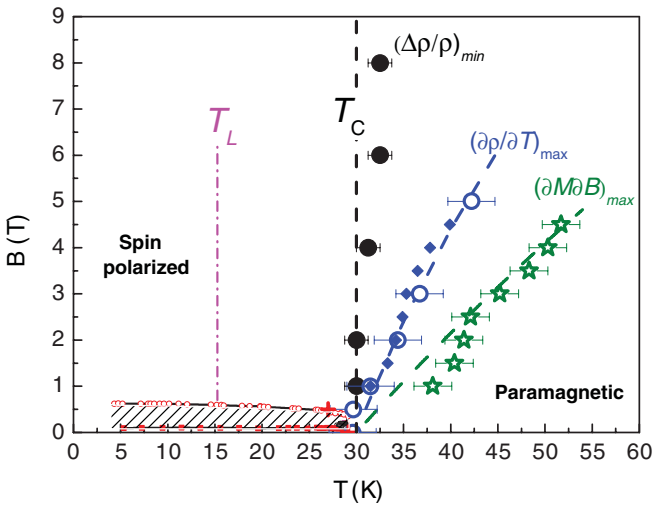

FIG. 4. (Color online) The magnetic phase diagram of MnSi restored from the experimental data. The hatched area marks helical phase, conical phase, and A phase, with the corresponding phase boundaries taken from the literature.[2,14] Points with error bars denote experimental positions of the $\partial\rho/\partial T$, $\partial M/\partial B$, and $\Delta\rho/\rho$ extrema; diamonds show result of simulations of $\partial\rho/\partial T$ with the help of experimental magnetization and resistivity data using Eq. (3). Dashed lines are the results of calculations with the help of the analytical model described in Sec. V. The dash-dotted line marks the position of the low-temperature anomaly.

of magnetic and transport properties agree rather well,[2,14,18,19] the critical SP-PM lines from $(\partial\rho/\partial T)_{\max}$, $(\partial M/\partial B)_{\max}$, and $(\Delta\rho/\rho)_{\min}$ data do not coincide. For example, a discrepancy between the positions of $(\partial M/\partial B)_{\max}$ and $(\Delta\rho/\rho)_{\min}$ extrema reaches ~10 K at 2 T and ~20 K at 5 T (Fig. 4). Therefore, there is no obvious reason for associating the SP-PM transition just with the maximum of $\partial M/\partial B$, as was previously supposed,[15] so the problem of the correct determination of this phase boundary appears to be nontrivial.

IV. MAGNETIC SCATTERING AND THE YOSIDA MODEL

The qualitative similarity between the evolution of $\partial M/\partial B$ and $\partial\rho/\partial T$ temperature dependences in magnetic fields (Figs. 1 and 2) suggests a certain link between resistivity and magnetization in MnSi. The negative sign of magnetoresistance also indicates the importance of magnetic scattering. The simplest theoretical description of negative magnetoresistance for a medium containing magnetic ions, on which band electrons are scattered, is given by Yosida's model.[17] The following relation between $\Delta\rho/\rho$ and M was obtained for a system with the s-d exchange:[17]

$$\Delta\rho/\rho = -a_0(S, y)(M/M_\infty)^2, \quad (1)$$

where M_∞ denotes the saturation value of magnetization. The coefficient a_0 in Eq. (1) depends on the spin S of the magnetic ion and the model parameter y, which is given by the ratio of the Fourier amplitudes of exchange energy J_0 and electrostatic

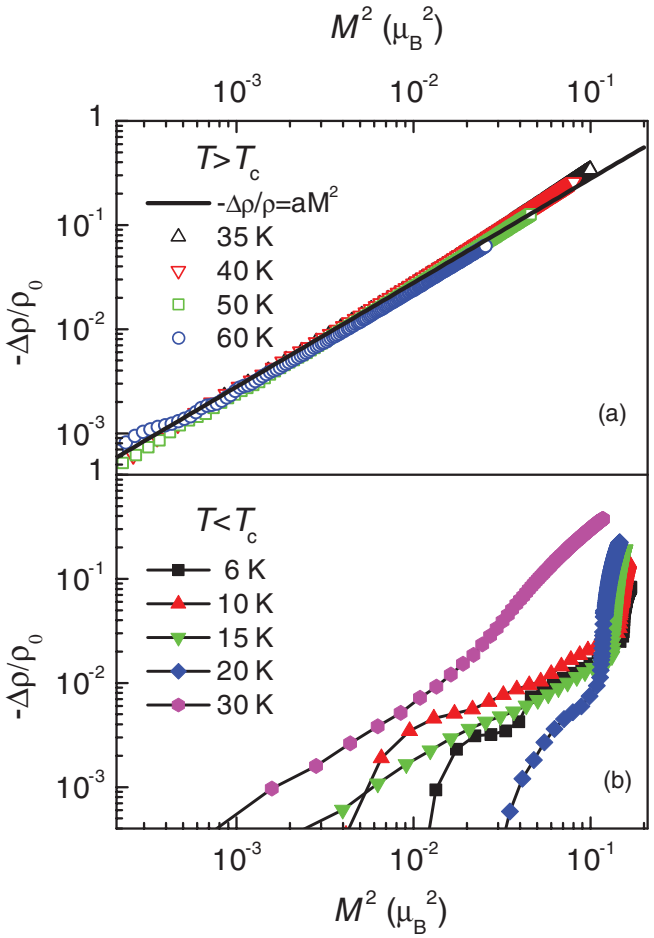

FIG. 5. (Color online) The absolute values of negative magnetoresistance versus the squared magnetization taken in μ_B per Mn ion: (a) the universal relation in PM phase ($T > T_c$) and (b) nonuniversal behavior in the SP phase ($T < T_c$). The straight line is the best fit for $T > T_c$.

scattering potential V_0: $y \sim (J_0/V_0)^2$.[17] For the spin $S = 1/2$ the expression for a_0 may be reduced to[17]

$$a_0 = y\frac{1 + 2/(1 + 3y/4)}{2(1 + 3y/4)}. \quad (2)$$

In this way, it is expected for the Yosida model that the temperature and field dependences of magnetoresistance are determined by temperature and field dependences of magnetization; i.e., for a material under consideration the relation between $\Delta\rho/\rho$ and M^2 should be linear and universal.

The plot of $-\Delta\rho/\rho$ as a function of M^2 for MnSi is shown in Fig. 5. The universal scaling suggested by Eq. (1) is valid for $T > 30$ K, whereas for lower temperatures the relation between the magnetoresistance and the squared magnetization becomes nonlinear and nonuniversal. It is worth noting that in the range $T > 30$ K the linear relation between $\Delta\rho/\rho$ and M^2 holds when $\Delta\rho/\rho$ varies by more than two orders of magnitude (Fig. 5). This result means that above 30 K in MnSi the magnetoresistance is predominantly controlled by magnetic scattering, and all other possible contributions to magnetoresistance are negligible. Moreover, a very good applicability of the Yosida model in the studied case forces us to revisit its physical grounds to elucidate the basic physics, which determines the high-field region of the magnetic phase diagram.

Before discussing this point, we wish to point out that the empirical relation $\Delta\rho/\rho = -aM^2$ allows us to find $\partial\rho/\partial T$ in a magnetic field by straightforward calculation of the derivative

$$\frac{\partial\rho(B,T)}{\partial T} = \frac{\partial\rho(0,T)}{\partial T}\{1 - a[M(B,T)]^2\} - 2a\rho(0,T)M(B,T)\frac{\partial M(B,T)}{\partial T}. \quad (3)$$

The above expression is valid as long as the maximum of $\partial\rho/\partial T$ occurs in the range $T > 30$ K (Fig. 4). Actually, using the $\rho(0,T)$ and $M(B,T)$ data and their derivatives (Figs. 1–2) as well as the value $a = 2.79 \pm 0.02\mu_B^{-2}$ determined from the slope of the universal dependence in Fig. 5, it is possible to calculate the position of the $\partial\rho/\partial T$ maximum for various magnetic fields. The result of the estimation (Fig. 4) demonstrates a perfect coincidence between experimental data (open circles) and the calculated results (filled diamonds). Therefore, it is reasonable to conclude that these two lines at the magnetic phase diagram [$(\partial\rho/\partial T)_{\max}$ and $(\partial M/\partial B)_{\max}$] are essentially the same due to the universal link between magnetoresistance and magnetization. However, the above analysis does not allow us to find a "true" boundary between the SP and PM phases.

In our opinion, the universal relation (1) appears as a consequence of the specific physical situation assumed within the Yosida model.[17] First, there are localized magnetic moments (LMMs), which scatter band electrons. Second, the scattering on LMMs is divided into two channels, one of which corresponds to the parallel alignment of electron spin and LMMs and another that corresponds to the antiparallel one. The scattering probability in the latter channel will decrease with the enhancement of magnetic field so that a lowering of temperature makes a scattering center more transparent, thus giving rise to negative magnetoresistance. Third, each localized magnetic moment acts as an individual independent scatter, and no interference occurs. Therefore, it is naturally to expect that magnetoresistance will depend on the average spin polarization rate M/M_∞ and, as magnetoresistance is the even function of magnetic field, the relation $-\Delta\rho/\rho \sim (M/M_\infty)^2$ should be valid, in agreement with the result of the exact calculation.[17]

At first glance the applicability of the aforementioned suggestion[17] to MnSi looks very surprising, and the validity of Eq. (1) and universal scaling (Fig. 5) cannot be foreseen. Indeed, the standard understanding of MnSi as an archetypal itinerant magnet with strong spin fluctuations seems to exclude any LMMs.[1] However, a recent study of magnetic resonance[16] showed that the physical picture in MnSi is in quantitative agreement with magnetic oscillations of Heisenberg-type LMMs, leaving a little room for any itinerant aspects of magnetism. This finding agrees well with the results of LDA calculations,[22] according to which the spin density in MnSi is localized on the Mn sites rather than being distributed over the unit cell. Therefore the presence of LMMs in MnSi could be considered to be at least a possible approximation. A more serious objection is the requirement of independent (noninterferent) scattering on LMMs. The Yosida model was

initially developed for the case of magnetic impurities, i.e., for a diluted case, where interference effects may be neglected.[17] At the same time four Mn^{4+} ($S = 1/2$) ions in the B20 unit cell cause the magnetic system to be apparently concentrated. In this respect, to satisfy the Yosida model validity requirements [confirmed by the good fitting of the experimental data using Eq. (1)], we need to postulate the local character of the interaction of the band electron with the magnetic center in the presence of strong coupling between free and localized spins.

Interestingly, the experimental value of $a = a_0/M_\infty^2 = 2.79$ together with $M_\infty \sim 0.4\mu_B$/Mn results in $y \approx 0.81$, which corresponds to $J_0/V_0 \sim 0.9$. This estimate shows that the magnetic interaction contribution to the scattering process is really strong for MnSi. It is worth noting that the above hypothesis agrees well with the qualitative model suggested in Ref. 16 in order to reconcile the possible experimental and theoretical evidence for LMMs with the facts supporting the presence of strong spin fluctuations in MnSi. In order to explain reduction of the saturated magnetic moment M_∞, it was supposed[16] that the bare magnetic moment of Mn^{4+} ($S = 1/2$) is screened by band electrons, which form a quasibound short-range spin-polaronic state in the vicinity of manganese magnetic ions. The transition rate between these states and band electrons is high and results in strong spin fluctuations, which, for instance, define the ESR line width.[16] Therefore the simplest process corresponding to the supposition[16] is a two-electron process wherein one band electron enters and another one leaves the vicinity of the magnetic center. The probability of such a process depends on the spin-polarization rate and, if the fine details of the LMM screening are omitted, could be considered to be a scattering process, which could be treated within the Yosida model.[17] However, in this case the parameter J_0 becomes an effective one and should be enhanced due to the formation of the quasibound state. The increase of the ratio J_0/V_0 leads to increase of the $\Delta\rho/\rho$ absolute values [Eqs. (1) and (2)] and agrees with the large negative magnetoresistance amplitude observed experimentally (Figs. 3 and 5).

The above arguments concerning the Yosida model applicability to the case of MnSi are valid when scattering processes on each Mn site are not correlated and controlled by an average spin-polarization rate; i.e., in the case of the PM phase. In the magnetically ordered phase the situation is very different.[17] In particular, it is reasonable to expect for the ferromagnetic phase that both localized and moving spins are already polarized. For that reason the basic assumption about two spin dependent scattering channels[17] fails, and magnetoresistance does not depend on spin states. As a result, the universal magnetoresistance scaling [Eq. (1)] is no longer valid, and any temperature dependence of the spin-dependent contribution to magnetoresistance in the SP phase is likely caused by thermal fluctuations destroying the "ideal" polarized state, so $\Delta\rho/\rho \to 0$ for $T \to 0$. Therefore, it is expected that in the PM phase the magnitude of the negative magnetoresistance in a fixed magnetic field first increases with decreasing temperature (as long as magnetization also increases), reaches a maximal absolute value at the transition between PM and SP phases, and then drops in the SP phase. In addition, a universal relation between magnetoresistance and magnetization holds in the PM phase.

Comparison with experiment shows that the aforementioned scenario exactly meets the case of MnSi. Indeed, the maximum of $-\Delta\rho/\rho$ is observed at $T_c \sim 30$–31 K (Fig. 3). Besides, the universal relation (1) is valid for $T > T_c$ (Fig. 5). At first glance such a coincidence is unexpected, as only the spin-dependent contribution to magnetization is considered. In metallic systems such as MnSi it is possible to expect a standard Drude-type positive magnetoresistance, estimated to be $\Delta\rho/\rho \sim (1/2)(\mu_H B)^2$ (here μ_H denotes the mobility of charge carriers). Our study of the Hall effect in MnSi showed that the mobility depends on temperature as $\mu_H \sim 1/T$, and hence the positive contribution to magnetoresistance can increase at low temperatures, compensating for the negative contribution and leading to formation of a $\Delta\rho/\rho = f(T)$ minimum. However, the absolute values of μ_H are very low, for example, $\mu_H(60\text{ K}) \approx 2$ cm^2/(V s) and $\mu_H(4.2\text{ K}) \approx 28$ cm^2/(V s). Thus for $B = 8$ T and $T < 60$ K the magnitude of the positive magnetoresistance is practically negligible, $\Delta\rho/\rho \sim (1/2)(\mu_H B)^2 \sim 2.5 \times 10^{-4}$–$1.2 \times 10^{-6}$, and therefore magnetic scattering dominates in MnSi. Consequently it is possible to associate the minimum of $\Delta\rho/\rho = f(T)$ with the transition between PM and SP phases, and therefore the corresponding phase boundary is almost vertical (Fig. 4). At temperatures above minimum the universal scaling $\Delta\rho/\rho = -a_0 M^2$ is observed, in agreement with the prediction of the Yosida model,[17] providing an additional argument in favor of the suggested interpretation.

Another interesting feature of the magnetoresistance temperature dependences is a shoulder of $\Delta\rho/\rho = f(T)$ observed at $T_L \sim 15$ K. This feature becomes more pronounced when magnetic field is increased [Fig. 3(b)]. Additionally, the shape of the $\Delta\rho/\rho = f(B)$ dependences changes for temperatures below 10 K, and a positive contribution to magnetoresistance is added to the negative one at low temperatures [Fig. 3(a)]. The above observations allow us to suggest that the regions of $T < T_L$ and $T_L < T < T_c$ are qualitatively different. In the framework of the approach used, this low-temperature anomaly may be explained by the change of spin polarization rate and hence may be related to some changes in the LMM system of MnSi.

V. MODELING THE MAGNETIC PHASE DIAGRAM

In order to check the idea about the field-independent PM-SP transition temperature T_c, we consider the simple model in which magnetization in the paramagnetic phase may be expressed as

$$M = M_\infty \tanh[\mu^* B/k_B(T - T_c)]. \quad (4)$$

The fitting of the experimental $M(B,T)$ curves shows that for $T > 30$ K and $B < 3$–5 T, Eq. (4) provides a reasonable approximation of experimental data with a constant value of $M_\infty \approx 0.28\mu_B$/Mn [see the black solid lines in Fig. 2(a)]. When $T_c = 30$ K is fixed, the parameter μ^* becomes a smooth function of temperature, increasing from $\mu^* \approx 4.9\mu_B$ at $T = 35$ K to $\mu^* \approx 5.7\mu_B$ at $T = 60$ K. It is worth noting that the combination $M_\infty \mu^*(T)/k_B$ reproduces within 5% accuracy the values of the Curie constant $C(T) = [\partial(\chi^{-1})/\partial T]^{-1}$ deduced from the temperature dependence of the MnSi magnetic susceptibility $\chi(T)$ in a weak magnetic field. This

finding confirms the correctness of the above approximation. However, both M_∞ and μ^* are nothing but model parameters, and their interpretation as any real physical quantities may be misleading.

It follows from formula (4) that position of the maximum of $\partial M/\partial B$ is given by

$$B_{\max} = z^* k_B (T - T_c)/\mu^*(T), \tag{5}$$

where $z^* = 0.772$ is the root of equation

$$z \tanh(z) = 1/2. \tag{6}$$

In order to calculate the $\partial\rho/\partial T$ maxima from Eq. (3), which already satisfies Yosida universal scaling, it is necessary to take into account derivatives $\partial\mu^*/\partial T$ and $\partial\rho(B = 0,T)/\partial T$. For simplicity we will assume linear approximations: $\rho = \rho_0(1 + T/T_\rho)$ with $T_\rho = 12.9$ K and $\mu^* = \mu_0(1 + T/T_\mu)$ with $T_\mu = 29.7$ K. These functional dependences follow from the linear fits of the resistivity at $T < 60$ K [dashed line in Fig. 1(a)] and of the model parameter $\mu^*(T)$. The position of the $\partial\rho/\partial T$ maxima will be again given by formula (5), but in this case z^* becomes a temperature-dependent root of the equation

$$\varphi(T) + z\left[\frac{1}{\tanh z \cosh^2 z} - 2\tanh z\right] = 0. \tag{7}$$

With the above linear approximations, Eq. (7) does not depend on any of parameters $a = a_0/M_\infty^2$, ρ_0, μ_0, and M_∞, and function $\varphi(T)$ acquires the form

$$\varphi(T) = 2[(T_\mu + T)/(T_\rho + T)][(T_\rho + T_c)/(T_\mu + T_c)].$$

The data calculated from Eqs. (4)–(7) together with the vertical phase boundary $T_c = \text{const}$ are shown in Fig. 4 by dashed lines. The suggested simple model reproduces well the experimental data. Consequently it is possible to conclude that the PM-SP phase boundary in MnSi may be almost vertical, as suggested by the qualitative analysis of the Yosida model, and could be associated with neither $\partial M/\partial B$ nor $\partial\rho/\partial T$ maxima. Moreover, this successful application of the simple interpolation (4) shows that the PM-SP transition in MnSi may be treated as occurring at well defined temperature T_c rather than as a broad crossover phenomenon as supposed previously.[15] At the same time the variation of the resistivity and magnetization in high magnetic field around T_c is smooth, and the singularity related with the denominator of the hyperbolic tangent may be observed only in the limit $B \to 0$.

VI. MAGNETIC RESONANCE AND LOCALIZED MAGNETIC MOMENTS

The above consideration supports the idea that the magnetic properties of MnSi are governed by Heisenberg-type LMMs rather than itinerant electrons. A similar supposition was made previously in Refs. 16 and 22. Particularly, a new technique for studying the magnetic resonance in strongly correlated metals developed in Refs. 20 and 21 was recently applied to investigate ESR in MnSi.[16] This method includes special geometry of cavity measurements and data analysis schema, which allow one to find the full set of spectroscopic parameters (g factor, line width, and the oscillating part of magnetization, M_{osc}). The latter quantity may be determined in absolute units,

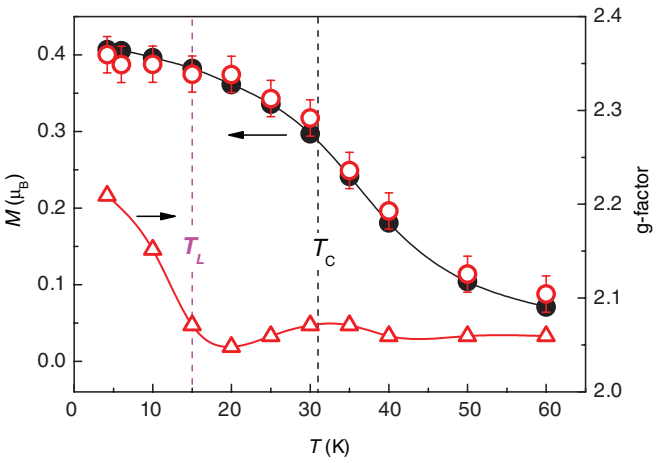

FIG. 6. (Color online) Static magnetization (open circles) and dynamic magnetization (filled circles) in μ_B per Mn ion, and g factor (open triangles) in MnSi. Lines are guides to the eye.

which distinguishes the new technique from standard ESR experiments.[20,21]

The ESR line-shape analysis performed in Ref. 16 suggests that in the whole temperature range uder investigation the observed magnetic oscillations are caused by LMMs, and possible spin diffusion is negligible. At the same time the temperature dependence of the line width exhibits a minimum at $T_c \sim 30$ K, which gives us way to connect this parameter with the magnitude of spin fluctuations in accordance with Moriya theory.[1,16] However, we report here some data processing errors found in Ref. 16, which are relevant to the problem of itinerant magnetism. In the present work (i) a computation error that affected g-factor values reported previously[16] is corrected and (ii) the temperature dependence of M_{osc}, which is missing in Ref. 16, is represented in comparison with the data of static magnetization M.

Measurements of magnetic resonance were carried out at frequency of $\sim$60 GHz; the resonant field was about $B_{\text{res}} \sim 2.2$ T. The results obtained are summarized in Fig. 6. For $T > 40$ K, the g factor does not depend on temperature: $g(T) = \text{const}$. This behavior agrees well with the localized nature of the oscillating magnetic moment in MnSi.[1,16] Around T_c ($20 < T < 40$ K) the $g(T)$ curve demonstrates a weak maximum, its amplitude being comparable with the error in the g-factor determination. Below $T \sim 15$–20 K the g factor starts to increase, showing $\sim$7% enhancement at 4.2 K.

The comparison of $M_{\text{osc}}(T)$ and static magnetization data at the resonant field $M(B_{\text{res}},T)$ indicates that these quantities coincide within experimental error in the whole temperature range $T < 60$ K where magnetic resonance may be detected. This observation deserves special discussion. Indeed, the equivalence of M_{osc} and M means that total spin density contributes to magnetic oscillations. So this situation seems to be natural for itinerant magnetism. In the case of MnSi the suggestion about LMMs means that there are two contributions to entire magnetization: one, M_{Mn}, results from the Mn LMMs, and another, M_{Pauli}, is induced by band electrons. Taking into consideration a standard expression for Pauli susceptibility

$\chi_{\text{Pauli}} = 3\mu_e^2 n_e/2E_F$, it is possible to obtain the following estimates:

$$\frac{M_{\text{Pauli}}}{M_{\text{Mn}}} \sim \frac{3}{2}\frac{n_e\mu_e^2}{Ck_B}\frac{k_B(T-T_c)}{E_{F0}}\frac{m^*}{m_0} \qquad (T > T_c) \qquad (8a)$$

and

$$\frac{M_{\text{Pauli}}}{M_{\text{Mn}}} \sim \frac{3}{2}\frac{n_e}{n_{\text{Mn}}}\left(\frac{\mu_e}{\mu_{\text{Mn}}}\right)\frac{\mu_e B_{\text{res}}}{E_{F0}}\frac{m^*}{m_0} \qquad (T < T_c). \qquad (8b)$$

Here C is the Curie constant for $T > T_c$; μ_e, n_e and μ_{Mn}, n_{Mn} are the magnetic moments and concentrations of band electrons and Mn ions, respectively; E_F stands for the Fermi energy $E_F \sim p_F^2/2m^*$; parameter $E_{F0} = E_F m_0/m^*$; p_F is the Fermi momentum; and m^* and m_0 are the effective masses of band and free electrons, respectively. It is supposed here that $M_{\text{Mn}} \sim n_{\text{Mn}}\mu_{\text{Mn}}$ saturates below T_c and the magnetization of the Mn ions follows the Curie-Weiss law $M_{\text{Mn}} \sim CB/(T - T_c)$ above T_c.

In MnSi the effective mass depends on temperature and increases with decreasing temperature from $m^* \sim 1.5m_0$ at $T = 75$ K to $m^* \sim 17m_0$ at $T = 10$ K.[23] As long as the contribution to magnetization from band electrons corresponds to the strongest spin fluctuations, it may not be observed in magnetic resonance measurements due to a strong broadening of the corresponding line width. The increase of $m^*(T)$ leads to the enhancement of M_{Pauli}, which may result in a difference between $M_{\text{osc}} = M_{\text{Mn}}$ and $M = M_{\text{Mn}} + M_{\text{Pauli}}$.

However, the calculation within Eqs. (8) does not confirm this hypothesis. For MnSi our measurements of the Hall effect result in $n_e/n_{\text{Mn}} = 0.89$, so that the parameter E_{F0} may be estimated as $E_{F0} \sim 4.1$ eV. Magnetization and magnetic susceptibility data suggest that the averaged value of the product Ck_B equals $1.66\mu_B^2$/Mn in the range $30 < T < 60$ K. Assuming $\mu_e \sim \mu_B$ and $\mu_{\text{Mn}} \sim 0.4\mu_B$ it is easy to find that $M_{\text{Pauli}}/M_{\text{Mn}} \sim 10^{-3}$ for the whole temperature range studied. Therefore, in the case when contributions from the LMMs and band electrons are treated separately, the total magnetization determined by the LMMs of Mn and M_{Pauli} is much less than the accuracy in evaluation of M_{osc} (Fig. 6).

Note that the real situation in MnSi may be more complicated than the scenario of Mn LMM screening by the band electrons, which is considered above (see Sec. V). This hypothesis allows estimation of the magnitude of the renormalized static magnetic moment for $T < T_c$. The Curie constant in the PM phase gives the value of LMM for a bare (unscreened) Mn $S = 1/2$ ion, $\mu_{\text{Mn}} = \sqrt{Ck_B/n_{\text{Mn}}} = 1.29\mu_B$, and the magnitude of the averaged value of screened Mn localized magnetic moment will be $\mu^* = \mu_{\text{Mn}} + \mu_B n_e/n_{\text{Mn}} \approx 0.4\mu_B$. This estimate is in good agreement with the low-temperature magnetization data for MnSi (Fig. 2) and thus the model suggested in Ref. 16 at least does not contradict the experiment. Moreover, based on a semiclassical approach[24] it is possible to show that the idea about a complex "composite" nature of Mn LMMs allows explanation of the dynamic magnetic properties of MnSi as well[16] including the observed weak variation of the g factor at the PM-SP phase boundary (Fig. 6). It is worth noting that there is only one magnetic contribution in the considered model for $T < T_c$. So the contribution of screened LMMs and hence the static and dynamic magnetizations should lead to $M = M_{\text{osc}}$ as observed experimentally (Fig. 6).

Therefore, it is possible to conclude that both itinerant magnetism and LMM models are consistent with our observations, in which M and M_{osc} coincide in SP and PM phases of MnSi. Some additional arguments are required for discrimination between these aforementioned possibilities. However, the analysis of ESR line shape,[16] the temperature independent g factor for $T > 15$ K (Fig. 6), and the good applicability of the Yosida model (Fig. 5) favor the explanation based on classical Heisenberg-type magnetism.

In concluding this section we wish to point out a correlation between the onset of the low-temperature growth of the g factor (Fig. 6) and the shoulder on the magnetoresistance temperature dependence at $T_L \sim 15$ K (Fig. 3). At the moment neither low-temperature changes in the g factor nor nonmonotonous $\Delta\rho/\rho$ dependence may be consistently interpreted in any models of MnSi magnetism. The low-temperature anomaly observed at $T_L \sim 15$ K could possibly correspond to a transition inside the SP phase. The nature of this possible transition requires additional clarification and will be discussed elsewhere.

VII. CONCLUSIONS

The study of the high-field region of the MnSi magnetic phase diagram shows that the temperature of the transition between PM and SP phases is well defined and is almost independent of magnetic field, equaling $T_c \sim 30$ K. As a result, the phase boundary $B_{SP}(T)$ appears to be practically vertical and has no positive slope as was suggested previously.[15] At the same time the broad maxima of the resistivity and magnetization derivatives, which develop in the range $T > T_c$, could not be associated with a "diffuse" SP-PM transition and appear to be due to the specific form of the functional dependences of these quantities in the PM phase. This experimental result is confirmed within a simple analytical model.

A universal relation between magnetoresistance and magnetization $\Delta\rho/\rho = -a_0 M^2$ found in the PM phase of MnSi holds in a wide range of temperatures and magnetic fields where magnetoresistance varies by more than two orders of magnitude. The observed behavior is shown to be explained by scattering of the band electrons on the Mn LMMs within the Yosida model.[17]

It is shown that the shape of the field dependences of magnetoresistance changes qualitatively in the SP phase of MnSi at $T_L \sim 15$ K, with the low-temperature g factor growing simultaneously below T_L. The nature of this low-temperature anomaly remains unclear, indicating the need for further development of the theory of magnetic properties of manganese monosilicide.

ACKNOWLEDGMENTS

The authors are grateful to S. M. Stishov and A. E. Petrova for helpful discussions. This work was supported by the Ministry of Education and Science of the Russian Federation (State program "Scientific and Pedagogical Personnel of Innovative Russia") and by the Russian Academy of Sciences (program "Strongly Correlated Electrons").

*demis@lt.gpi.ru
†National Science and Technology University (MISiS), 4 Leninskii av., 119049 Moscow, Russia.

[1]T. Moriya, *Fluctuations in Itinerant Electron Magnetism* (Springer-Verlag, Berlin, 1985).
[2]Y. Ishikawa, G. Shirane, J. A. Tarvin, and M. Kohgi, Phys. Rev. B **16**, 4956 (1977).
[3]T. Sakakibara, H. Mollymoto, and M. Date, J. Phys. Soc. Jpn. **51**, 2439 (1982).
[4]Y. Ishikawa, Y. Noda, Y. J. Uemura, C. F. Majkrzak, and G. Shirane, Phys. Rev. B **31**, 5884 (1985).
[5]S. V. Maleyev, Phys. Rev. B **73**, 174402 (2006).
[6]S. V. Grigoriev, S. V. Maleyev, A. I. Okorokov, Yu. O. Chetverikov, P. Boni, R. Georgii, D. Lamago, H. Eckerlebe, and K. Pranzas, Phys. Rev. B **74**, 214414 (2006).
[7]S. V. Grigoriev, S. V. Maleyev, A. I. Okorokov, Yu. O. Chetverikov, and H. Eckerlebe, Phys. Rev. B **73**, 224440 (2006).
[8]S. V. Grigoriev, S. V. Maleyev, E. V. Moskvin, V. A. Dyadkin, P. Fouquet, and H. Eckerlebe, Phys. Rev. B **81**, 144413 (2010).
[9]D. Belitz, T. R. Kirkpatrick, and J. Rollbuhler, Phys. Rev. Lett. **94**, 247205 (2005).
[10]A. E. Petrova, V. Krasnorussky, J. Sarrao, and S. M. Stishov, Phys. Rev. B **73**, 052409 (2006).
[11]A. E. Petrova, V. N. Krasnorussky, T. A. Lograsso, and S. M. Stishov, Phys. Rev. B **79**, 100401(R) (2009).
[12]C. Pappas, E.Lelievre-Berna, P. Falus, P. M. Bentley, E. Moskvin, S. Grigoriev, P. Fouquet, and B. Farago, Phys. Rev. Lett **102**, 197202 (2009).
[13]C. Pappas, E. Lelievre-Berna, P. Bentley, P. Falus, P. Fouquet, and B. Farago, Phys. Rev. B **83**, 224405 (2011).
[14]A. Neubauer, C. Pfleiderer, B. Binz, A. Rosch, R. Ritz, P. G. Niklowitz, and P. Boni, Phys. Rev. Lett. **102**, 186602 (2009).
[15]C. Thessieu, C. Pfleiderer, F. N. Stepanov, and J. Flouquet, J. Phys. Condens. Matter **9**, 6677 (1997).
[16]S. V. Demishev, A. V. Semeno, A. V. Bogach, V. V. Glushkov, N. E. Sluchanko, N. A. Samarin, and A. L. Chernobrovkin, JETP Lett. **93**, 213 (2011).
[17]K. Yosida, Phys. Rev. **107**, 396 (1957).
[18]S. Stishov, A. E. Petrova, S. Khasanov, G. Kh. Panova, A. A. Shikov, J. C. Lashley, D. Wu, and T. A. Lograsso, Phys. Rev **76**, 052405 (2007).
[19]D. Lamago, R. Georgii, and P. Boni, Physica B **359–361**, 1171 (2005).
[20]A. V. Semeno, V. V. Glushkov, A. V. Bogach, N. E. Sluchanko, A. V. Dukhnenko, V. B. Fillippov, N. Yu. Shitsevalova, and S. V. Demishev, Phys. Rev. B **79**, 014423 (2009).
[21]S. V. Demishev, A. V. Semeno, A. V. Bogach, N. A. Samarin, T. V. Ishchenko, V. B. Filipov, N. Yu. Shitsevalova, and N. E. Sluchanko, Phys. Rev. B **80**, 245106 (2009).
[22]M. Corti, F. Carbone, M. Filibian, Th. Jarlborg, A. A. Nugroho, and P. Carretta, Phys. Rev. B **75**, 115111 (2007).
[23]F. P. Mena, D. van der Marel, A. Damascelli, M. Fath, A. A. Menovsky, and J. A. Mydosh, Phys. Rev. B **67**, 241101(R) (2003).
[24]R. K. Wangsness, Phys. Rev. **91**, 1085 (1953).